A novel adaptive mechanical-wetting lens for visible and near infrared imaging

Su Xu[1], Yifan Liu[1], Hongwen Ren[1, 2,3] and Shin-Tson Wu[1,*]

[1]*College of Optics and Photonics, University of Central Florida, Orlando, Florida 32816, USA*
[2]*Department of Polymer Nano-Science and Engineering, Chonbuk National University, Chonju, Chonbuk, 561-756, Republic of South Korea*
[3]*hongwen@jbnu.ac.kr*
**swu@mail.ucf.edu*

Abstract: We demonstrate an adaptive mechanical-wetting lens with a concentric reservoir to reduce image aberrations and overcome the gravity effect. This lens adopts liquid pressure to change the interface between two immiscible liquids which, in turn, changes the focal length of the resultant liquid lens. Good optical performance, high resolution, and a wide dynamic range of both positive and negative optical power are achieved. Since no PDMS is employed, such lenses can extend their working range to infrared region by choosing proper liquids.

©2010 Optical Society of America

OCIS codes: (010.1080) adaptive optics; (220.3620) lens design

References and links

1. S. Reza, and N. A. Riza, "A liquid lens-based broadband variable fiber optical attenuator," Opt. Commun. **282**(7), 1298–1303 (2009).
2. S. Murali, K. P. Thompson, and J. P. Rolland, "Three-dimensional adaptive microscopy using embedded liquid lens," Opt. Lett. **34**(2), 145–147 (2009).
3. N. Sugiura, and S. Morita, "Variable-focus liquid-filled optics lens," Appl. Opt. **32**(22), 4181–4186 (1993).
4. H. Ren, and S. T. Wu, "Variable-focus liquid lens," Opt. Express **15**(10), 5931–5936 (2007).
5. D. Zhang, V. Lien, Y. Berdichevsky, J. Choi, and Y. H. Lo, "Fluidic adaptive lens with high focal length tunability," Appl. Phys. Lett. **82**(19), 3171–3173 (2003).
6. C. A. López, C. C. Lee, and A. H. Hirsa, "Electrochemically activated adaptive liquid lens," Appl. Phys. Lett. **87**(13), 134102–134104 (2005).
7. L. Miccio, A. Finizio, S. Grilli, V. Vespini, M. Paturzo, S. De Nicola, and P. Ferraro, "Tunable liquid microlens arrays in electrode-less configuration and their accurate characterization by interference microscopy," Opt. Express **17**(4), 2487–2499 (2009).
8. L. Dong, A. K. Agarwal, D. J. Beebe, and H. Jiang, "Adaptive liquid microlenses activated by stimuli-responsive hydrogels," Nature **442**(7102), 551–554 (2006).
9. M. Vallet, B. Berge, and L. Volvelle, "Electrowetting of water and aqueous solutions on poly (ethylene terephthalate) insulating films," Polymer (Guildf.) **37**(12), 2465–2470 (1996).
10. C. C. Cheng, and J. A. Yeh, "Dielectrically actuated liquid lens," Opt. Express **15**(12), 7140–7145 (2007).
11. S. Xu, Y. J. Lin, and S. T. Wu, "Dielectric liquid microlens with well-shaped electrode," Opt. Express **17**(13), 10499–10505 (2009).
12. T. Shin, C. Chen, J. Ho, and F. Chuang, "Fabrication of PDMS microlens and diffuser using replica molding," Mirco. Eng. **83**(11–12), 2499–2503 (2006).
13. S. Kuiper, and B. H. W. Hendriks, "Variable-focus liquid lens for miniature cameras," Appl. Phys. Lett. **85**(7), 1128–1130 (2004).
14. H. Oku, and M. Ishikawa, "High-speed liquid lens with 2 ms response and 80.3 nm root-mean-square wavefront error," Appl. Phys. Lett. **94**(22), 221108 (2009).
15. S. T. Wu, "Absorption measurements of liquid crystals in the ultraviolet, visible, and infrared," J. Appl. Phys. **84**(8), 4462–4465 (1998).
16. C. G. Tsai, C. N. Chen, L. S. Cheng, C. C. Cheng, J. T. Yang, and J. A. Yeh, "Planar liquid confinement for optical centering of dielectric liquid lenses," Photon. Technol. Lett. **21**(19), 1396–1398 (2009).
17. D. Zhu, C. Li, X. Zeng, and H. Jiang, "Tunable-focus microlens arrays on curved surfaces," Appl. Phys. Lett. **96**(8), 081111–081113 (2010).
18. C. G. Schroer, M. Kuhlmann, U. T. Hunger, T. F. Günzler, O. Kurapova, S. Feste, F. Frehse, B. Lengeler, M. Drakopoulos, A. Somogyi, A. S. Simionovici, A. Snigirev, I. Snigireva, C. Schug, and W. H. Schröder, "Nanofocusing parabolic refractive x-ray lenses," Appl. Phys. Lett. **82**(9), 1485 (2003).

#126235 - $15.00 USD Received 30 Mar 2010; revised 19 May 2010; accepted 19 May 2010; published 26 May 2010

1. Introduction

Adaptive lenses are attractive for vision application, image processing, beam steering, and portable electronic devices [1–10]. Several approaches, such as fluidic pressure [3–5], electrochemistry [6], thermal effect [7], environmentally adaptive hydrogel [8], electro-wetting [9] and dielectrophoresis [10,11], have been developed to tune the focal length. Nowadays, most adaptive lenses are working in the visible region. Due to great potential in military and commercial applications, adaptive lenses working in infrared (IR) region are in high demand.

In a typical membrane liquid lens based on fluidic pressure, at least one surface of the lens is made of elastic membrane which acts as a deformable surface. Its focal length is controlled by pumping liquid in and out of the lens chamber which changes the curvature of the liquid lens accordingly [3–5]. This kind of liquid lens exhibits a very wide dynamic range. Polydimethylsiloxane (PDMS) membrane is commonly employed because of its super elasticity and good transmittance in visible and near IR region [12]. However, the gravity effect exists in any elastic membrane lens when it is placed in vertical position, which may cause an asymmetric shape and degrade the image performances. Making high quality PDMS membrane and uniformly installing it on the lens frame are also challenging. All these factors limit the optical performances of elastic membrane lenses.

Electro-wetting lens [13] is another popular liquid lens driven by an electric field. In this lens, a conducting liquid drop forms a contact angle on a solid surface, and it is surrounded by another immiscible insulating fluid. The contact angle can be tuned if a suitable voltage is applied across the liquid and the counter-electrode underneath the solid surface, which leads to a shape change of the droplet and a corresponding change in focal length [9]. In comparison with elastic membrane lens, electro-wetting lens is insensitive to shocks and vibrations if the two liquids match in density, and it exhibits a very smooth liquid-liquid interface (nanoscale) because of the surface tension. However, electrolysis, Joule heating, and microbubbles often occur in electro-wetting lenses due to the transportation of the free electric charges and the alternating electric fields [10].

In this paper, we demonstrate an adaptive mechanical-wetting lens to keep the advantages of smooth liquid-liquid interface and minimum gravity effect while overcoming the shortcomings of an electric-wetting lens. Our lens uses liquid pressure to change the interface between two immiscible liquids, which in turn changes the focal length of the resultant liquid lens. We call this device as mechanical-wetting lens because it involves two liquids in a lens cell, similar to that in an electro-wetting lens, while the liquid-liquid interface is changed by a mechanical force. In comparison with the design whose reservoir is on one side of the lens area [14], our new design pumps liquid uniformly through the entire periphery of the lens area because of the concentric reservoir. It eliminates the gradient effect in liquid pressure and stabilizes the optical performance during the transition process. Furthermore, since no PDMS is employed, our lens can expand its working range to IR. To prove concept, we show the performance of our lens at $\lambda = 1310$ nm.

2. Device structure and analysis

Figure 1 shows the device structure of the mechanical-wetting lens. From top to bottom, the lens frames consist of a top cap, a reservoir body, and a bottom cap, as shown in Fig. 1(a). There are two holes in the reservoir body. An observation hole covered by glass is in the center of the reservoir body, and a ring-shaped hole covered by elastic membrane (marked in blue) is concentric with the observation hole, they are connected with each other through tiny linkages. Two immiscible liquids interface at an aperture hole in the middle circular slab (marked in green), as shown in Fig. 1(b). The top and bottom caps are the driving devices to press the membrane. Each cap is a cylindrical shell with one end open and the other end closed, as shown in Fig. 1(c), and a hole is drilled in the closed end for observation. The screw threads on the inside wall of each cap match those on the outside wall of the reservoir body.

#126235 - $15.00 USD Received 30 Mar 2010; revised 19 May 2010; accepted 19 May 2010; published 26 May 2010
(C) 2010 OSA

Thus when the cap is screwed toward the reservoir body, the bump in the cover (marked in red) will press the elastic membrane, causing the liquid-liquid interface to bend.

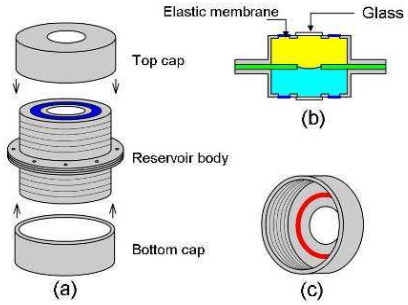

Fig. 1. Device structure of a mechanical-wetting lens: (a) Assembled system, (b) Side view of the reservoir body, and (c) Cap with a bump inside.

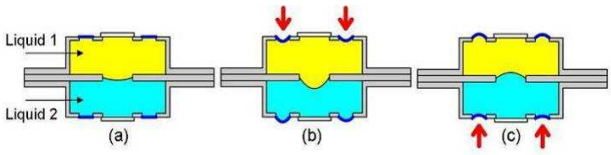

Fig. 2. Side view of a mechanical-wetting lens structure in: (a) Initial state, (b) Further positive state, and (c) Negative state.

Figure 2 shows the cross-sectional view of the reservoir body in different driving states. At the initial state, assuming the top and bottom elastic membranes are both flat, liquid-2 forms a concave shape at the aperture hole in the middle layer because of the surface tension, as Fig. 2(a) shows. The liquid lens behaves as a positive lens if the refractive index of liquid-1 is larger than that of liquid-2. When an external pressure is applied to the top elastic membrane, because the volume of the liquids are not constringent, liquid-1 in the lens chamber is redistributed, pressing the interface to change its shape to further concave, as shown in Fig. 2(b), and the optical power of the resultant lens goes further positive. If an external pressure is applied to the bottom elastic membrane, liquid-2 in the lens chamber is redistributed, pressing the interface to change its shape from concave to convex with an increasing external pressure, as shown in Fig. 2(c), accordingly the optical power of the resultant lens changes from positive to negative.

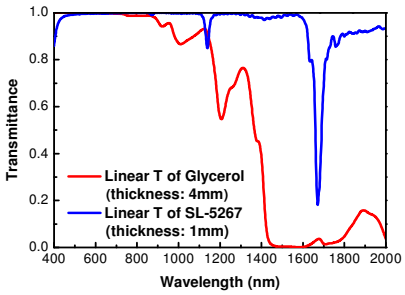

Fig. 3. Transmission spectra of SL-5267 and Glycerol measured from 400 nm to 2000 nm.

The two liquid employed in Ref. [14]. are ultrapure water (n_1 = 1.33) and PDMS gel (n_2 = 1.40), the refractive indices difference is small and the water is easy to evaporate, causing a short device lifetime. To overcome these drawbacks, Glycerol (from Sigma-Aldrich, n = 1.474 at λ = 550 nm and 1.460 at 1293 nm, surface tension = 64 mN/m@20°C and ρ = 1.25 g/cm^3) and SantoLight Optical Fluids SL-5267 (from Santovac® Fluids, n = 1.670 at

#126235 - $15.00 USD Received 30 Mar 2010; revised 19 May 2010; accepted 19 May 2010; published 26 May 2010
(C) 2010 OSA

λ = 550 nm and 1.635 at 1310 nm, surface tension = 50 mN/m@20°C and ρ = 1.2 g/cm^3) are used. These two immiscible liquids have similar density to minimize the gravity effect and a large refractive index difference. They also show good transmittance in both visible and near IR regions, which enables our lens to work in near IR. Figure 3 shows the measured transmission spectra of these two liquids. The dramatic drop in the transmission spectra of SL-5267 near 1650 nm is due to the overtone absorption of CH/CH_2/CH_3 stretching bands which occur in 3.3-3.5 μm. Thus, its second harmonic appears at ~1.65-1.75 μm [15].

While making a lens described in Ref. [14]. using Optical Fluids SL-5267 and Glycerol, we found this design could keep a uniform liquid-liquid interface only if the transition time was slow (a few tens of seconds). If the transition time was reduced to a few seconds, then the liquid interface change was no longer uniform and a severe image aberration appeared during the transition process. The aberration became even worse as the aperture increased. The reason is explained as follows: when actuated in high speed, the pressure increases quickly so that a pressure gradient builds up from the reservoir area to the lens area. As a result, the liquid interface first bends on the high pressure end (near the reservoir) and then propagates to the other end. This gradient effect not only induces image aberration during the transition process, but also creates high stress on one end of the interface, resulting an interface movement and device instability. This problem originates from the high viscosity of Glycerol. Our solution is to make a lens with a concentric reservoir, as depicted in Fig. 1. Thus, the pressure gradient will be significantly suppressed, because the pressure along the entire periphery of the liquid-liquid interface is almost the same.

3. Experiment

The lens frames were made of aluminum. The two chambers in the reservoir body and the middle slab were connected with each other by screws and sealed by silicon glue to prevent fluid leakage. Then, two liquids were filled into each chamber, the upper chamber was filled by Optical Fluids, and the lower was Glycerol. The amount of each filled liquid was well controlled so that their interface stayed at the aperture hole of the middle layer. Some lubricate was added to the outer surface of the elastic membranes in order to reduce the friction when the caps were pressing the membranes. Coaxial design is desired in order to maintain optical functions of a liquid lens [16]. When the parts were machined on the lathe, they were all aligned to the same axis. Six screws holes were drilled in the reservoir body and the central layer respectively, and screws were used to connect and align these parts precisely. The diameter of the observation hole and aperture hole is 5 mm and 4 mm, respectively. The inner and outer diameter of the ring-shaped hole covered by elastic membrane is 20 mm and 28 mm, respectively. The middle slab is ~1 mm thick, the rubber bump is ~2 mm thick and each liquid layer is ~4 mm thick. The total thickness of the whole device is ~15 mm, and it can be further reduced if thinner frames are used. The screw pitch is 1/32 inch, which means the bump goes towards the reservoir body 1/32 inch when the cap is rotated in one full circle. The lens was tested in the visible region and near IR region.

4. Results and discussions

To evaluate the lens performances during transition process, we recorded the image of an object through the liquid lens under white light. A picture, printed “5” was set very close to the lens, and a CCD camera was used to record the image change. Figure 4 shows the images taken through the lens at three different focusing states corresponding to those in Fig. 2. Firstly, the lens was in the initial state with a positive optical power and the observed image was upright, virtual, and magnified, as shown in Fig. 4(a), because the distance between the object and the lens cell was shorter than the focal length. When the top cap was screwed towards the reservoir body, the rubber bump touched the elastic membrane on the top chamber and pushed it to go deeper with an increasing traveling distance, and consequently the resultant lens became further positive and the image size was further magnified, as shown in Fig. 4(b). The resultant liquid lens began to exhibit less positive and then negative optical power when the bottom cap was screwed toward the reservoir body with an increasing

#126235 - $15.00 USD Received 30 Mar 2010; revised 19 May 2010; accepted 19 May 2010; published 26 May 2010
(C) 2010 OSA

traveling distance, and the observed image was reduced, as shown in Fig. 4(c). A tiny image aberration was observed at the border of the aperture, because the aperture was not perfectly circular, and the defects in the circumference of the aperture hole introduced the image aberration. If the middle slab and the aperture hole can be made in high precision, e.g., fabricated by photolithography, a much smaller wavefront error will arise in the lens border [14]. To visually observe the transition process between positive and negative optical power, a movie was taken, as shown in Fig. 4(d). The image changed continuously and uniformly during the top cap's traveling, and no obvious aberration was observed. The lens' resolution was also measured by the microscope. Figure 4(e) shows the image of a 1951 U.S. Air Force (USAF) resolution target taken in the transmission mode of the microscope under green illumination. The highest resolution of the device is ~203 lp/mm as the patterns of group 7 number 5 are still resolvable.

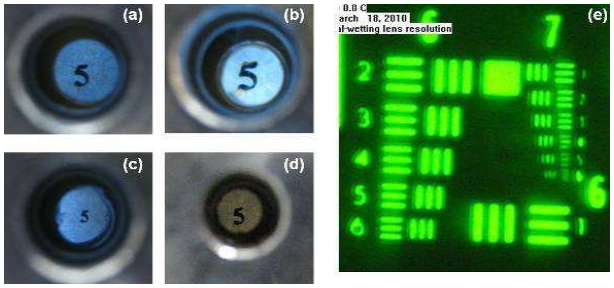

Fig. 4. Images taken through the lens in: (a) Initial state, (b) Further positive state, (c) Negative state, (d) Lens' transition states from positive power to negative power (Media 1),and (e) Len's resolution at the initial state.

To measure the back focal distance (BFD) of the liquid lens, we expanded and collimated a He-Ne laser beam (λ = 633 nm) to ~10 mm in diameter and let it normally pass through the liquid lens. For the positive lens, the focal point was determined by the smallest focused point (a quite circular point with a diameter of ~1 mm) of the collimated input beam along the optic axis, as shown in Fig. 5(a). For the negative lens, BFD was determined by a geometrical imaging method, as Fig. 5(b) shows. Every measurement was repeated three times and the results were averaged. When the bottom cap is moving towards the reservoir body, the traveling distance dependent BFD is depicted in Fig. 5(c), here P (1/32 inch) stands for the screw pitch.

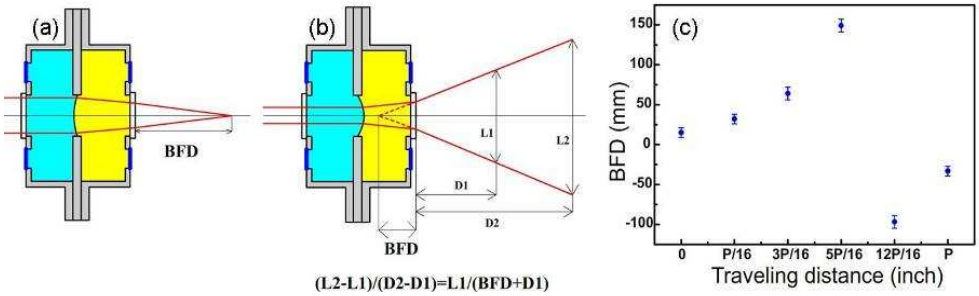

Fig. 5. (a) BFD measurement of the positive lens, (b) BFD measurement of the negative lens, and (c) Measured BFD vs. traveling distance of the bottom cap.

The lens' ability and performance for near IR imaging are also evaluated. The experimental setup is shown in Fig. 6(a). An IR fiber laser (λ = 1300 nm) was collimated and then illuminated the mechanical-wetting lens. A fluorescent card was used as a screen for observation. The lens was set vertically and some light spot images were recorded. The screen was set at the focus of the testing lens in the initial state, at first, a tiny and bright spot was observed due to the lens' initial positive optical power, as shown in Fig. 6(b), when the

#126235 - $15.00 USD Received 30 Mar 2010; revised 19 May 2010; accepted 19 May 2010; published 26 May 2010
(C) 2010 OSA

bottom cap was screwed toward the reservoir body, the lens first went less positive, then flat and finally negative. Thus the light spot was gradually increased, as shown in Figs. 6(c)-6(d). The spot is quite circular, and the light is highly centrally focused without any obvious noise when observed in the dark background. Due to absorption of Glycerol, the total lens transmittance is estimated to be ~60% under 1310 nm illumination.

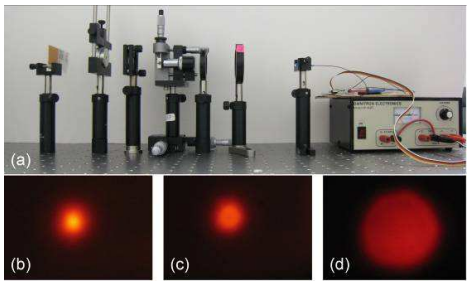

Fig. 6. (a) Experimental setup for lens testing under 1310nm illumination, Light spots taken in: (b) Initial state, (c) Less positive state, and (d) Negative state (Media 2)

Our simple mechanical-wetting lens is working well in visible and near IR regions. It paves a way to fabricate an adaptive liquid lens for mid-IR, long-IR or even UV imaging, by choosing proper liquids with good transmittance in the desired spectral region. Besides, some other criteria should be taken into consideration, e.g., density matching, large refractive indices difference, immiscibility, non-volatility, and stability. A matched density helps to minimize the gravity effect and realize highly axis-symmetric liquid droplet, especially for large aperture lenses. Large refractive index difference could enhance the optical power, while the non-volatility and good stability are crucial for lengthening the device lifetime. Furthermore, surface treatment can be applied to the middle slab, e.g., hydrophobic-hydrophilic bond, helps to confine the position of the liquids interface on the aperture hole [17], and other surface treatment may help to control the shape of the interface. If a parabolic shape could be obtained, the lens' spherical aberration could be reduced [18]. The tuning step is determined by the screw pitch on the outside wall of the reservoir body and inside wall of the caps. Thus, a smaller screw pitch would be favored for finer tuning. The present structure is favorable for self-adjustment in vision applications; for those applications in need of automatic driving and fast response, a mechanical motor can be adopted.

5. Conclusion

An adaptive mechanical-wetting lens for visible and near IR imaging is demonstrated. Benefiting from the concentric reservoir structure and smooth liquid-liquid interface, the lens' transition process is smooth, and the optical performance is quite good and stable. When the bottom cap is traveling in one full circle, the back focal distance can be changed from infinity to ~15 mm and from −33.3 mm to infinity under 633 nm illumination, both positive and negative optical power can be obtained. Under 1310 nm illumination, the lens shows a ~60% transmittance and tunable light spots with circular shape could be observed. Mechanical motor would help to achieve automatic driving and fast response. Fine processing and surface treatment could further improve the lens' performances. The same device concept can be extended to mid-IR and long-IR, provided that proper transparent liquids are employed.

Acknowledgements

The authors are indebted to H. Xianyu and N. Bai for their technical assistance and useful discussions, and AFOSR for partial financial support under Contract No. FA95550-09-1-0170.

#126235 - $15.00 USD Received 30 Mar 2010; revised 19 May 2010; accepted 19 May 2010; published 26 May 2010
(C) 2010 OSA